Comparative Study of Transmission Expansion Planning with Conventional and Unconventional High Surge Impedance Loading (HSIL) Lines

Bhuban Dhamala
Dept. of Electrical and Computer Engineering
The University of Texas at Dallas
Richardson, TX, USA
bhuban.dhamala@utdallas.edu

Mona Ghassemi
Dept. of Electrical and Computer Engineering
The University of Texas at Dallas
Richardson, TX, USA
mona.ghassemi@utdallas.edu

2024 IEEE Power & Energy Society General Meeting (PESGM) | 979-8-3503-8183-2/24/$31.00 ©2024 IEEE | DOI: 10.1109/PESGM51994.2024.10689086

***Abstract*— The strategic planning of transmission expansion is paramount in ensuring the reliability and efficiency of power systems, particularly in the context of growing electricity demand and the integration of renewable energy sources. This paper investigates the utilization of unconventional high surge impedance loading (HSIL) lines in transmission expansion planning (TEP) and offers a comparative analysis of their performance against conventional line-based TEP methods. Commencing with a 17-bus 500 kV test system known for its robust operation under normal and all single contingencies at different loading scenarios, the objective is to connect a new load at a new location. Meticulously examining and comparing the number of lines and right of way (ROW) required for both methods while maintaining uniform conductor weight per circuit, the effectiveness of unconventional HSIL lines within the TEP context is assessed.**

Keywords—Transmission expansion planning, power system planning, unconventional high surge impedance loading lines.

I. Introduction

In the dynamic power industry, restructuring has revolutionized demand and generation. Despite incorporating energy-saving technologies and demand response, load demand is on the rise. The Western Electricity Coordinating Council (WECC) 2022 report [1] forecasts an 11.4% surge in collective demand across the entire U.S. Western connection from 2023 to 2032. Future generations will undergo a notable shift, with renewables taking the lead due to state-mandated Renewable Portfolio Standards for decarbonization [2], compelling utilities to source a specified portion of their electricity from renewable sources. With the persistent surge in energy demand and increasing integration of large-scale renewable resources into the primary power grid, development of a robust and reliable power grid is essential. A study conducted in 2021 regarding net zero emission in the United States by 2050 found that the high voltage transmission line capacity would need to increase by approximately 60% by 2030 and triple by 2050 [3]. However, the transmission sector, which serves as the highway for transporting electricity within power systems, has seen limited hardware changes in power industry history.

In the realm of electrical power transmission, overhead lines have been a dominant and influential power transportation method, set to continue its prevalence. Despite the availability of underground cables as an alternative, the substantial cost difference, often three to ten times higher, particularly at high voltage levels, limits its widespread adoption [4, 5]. Furthermore, high-voltage AC cables pose technical challenges due to their high charging current. The necessity of HVDC transmission for bulk power transmission, along with its technologies and recent developments, is outlined in [6, 7]. However, economically, it proves feasible only for very long distances, typically exceeding 800 km [7]. A significant boost in transmission line capacity is imperative to accommodate the upcoming shifts in the power industry. Limitations of conventional lines such as substantial costs on upgrading lines, acquiring large ROW for new lines, and environmental impact on expanding line corridors underscore the need for advanced transmission technologies. HSIL lines present a promising alternative to the conventional line. A comprehensive review of HSIL lines, evaluating technical gaps and outlining the ways for future research, has been illustrated in [8]. Paper [9] explores compact transmission lines with different conductor bundles, examining SIL, impact of each phase on ground surface electric field intensity, and conductor surface gradient. Valuable insights from the implementation of HSIL lines in Brazil are detailed in [10], highlighting two key geometric factors for improving SIL – compacting phases and expanding conductor bundles. In the study [11], conventional high surge impedance loading lines are investigated, featuring symmetrically positioned subconductors on a circle across all phases. This study uncovers a significant correlation between surge impedance loading and the uniformity of electric field. This paper presents an unconventional HSIL line configuration, featuring eight subconductors per bundle, where the subconductors of outer phases are arranged in a generic disposition, and the center phase follows an almost circular arrangement. The paper then conducts a comparative study on TEP within a 500 kV test system. The primary focus of the TEP is to supply power to a new location using two different transmission line technologies, the conventional lines and the proposed unconventional HSIL lines, maintaining almost identical total aluminum cross-section of conductors and weight per unit length for both lines. The study evaluates system performance under various loading conditions – peak load, dominant load (60% of peak load), and light load (40% of peak load) – and should be operable under normal and all single contingency conditions.

This work was supported in part by the National Science Foundation (NSF) under Award #2306098.

II. Information on Test System for TEP

A. Power System Topology

Fig.1 depicts a single-line representation of the 500 kV, 17-bus test system. Specifically, bus 1 acts as the swing bus, while buses 3, 6, 8, 10, 12, 13, and 15 are voltage-controlled buses (PV buses), with the rest buses serving as load buses (PQ buses). The length of each transmission line is presented in Table I. It should be noted that buses 1 and 2 are connected by two lines and the length presented in Table I is the length of each line. This is the case for other double-line connections.

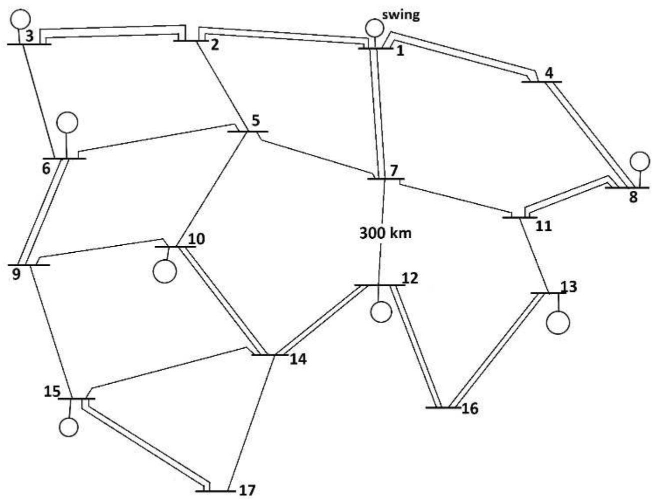

Fig. 1. Single line diagram of the 17-bus test system for TEP studies.

TABLE I. LENGTH OF TRANSMISSION LINES IN THE 17-BUS TEST SYSTEM

Line	Length(km)	Line	Length (km)
1-2	410.32	7-12	300.00
1-4	426.77	8-11	349.09
1-7	370.91	9-10	447.27
2-3	436.90	9-15	398.18
2-5	294.55	10-14	392.73
3-6	349.55	11-13	261.29
4-8	416.13	12-14	348.38
5-6	415.00	12-16	406.45
5-7	435.48	13-16	417.27
5-10	376.36	14-15	458.18
6-9	316.36	14-17	403.64
7-11	387.09	15-17	402.16

B. Transmission Line Configuration

Fig. 2 depicts the geometric arrangement of 500 kV transmission lines in the test system adopting a horizontal configuration with a phase spacing of 12.3 m at a height of 28 m. Each phase includes four bundled sub-conductors (red dot). The conductor specifications and calculated line parameters for this configuration are presented in Table II. The surge impedance loading of this line is 996.12 MW.

C. Generation, Load, and Shunt Compensation at Peak Load

Generation, load, and shunt compensation information at peak load for each bus are presented in Table III. For all generating units, voltage magnitude, |V|=1.05 p.u., and for slack bus, voltage angle, δ_1=0. A typical assumption during load flow studies is to consider Q_{gmax}= 0.6P_g and Q_{gmin}= -0.3P_g. The test system consists of 16 loads connected to all buses except the slack bus. It is assumed that loads operate at a power factor of 0.9 lagging. In addition, the system also incorporates fixed shunt capacitors that are connected to different buses. The total capacity of connected shunt capacitors is 1100 Mvar. Details of this test system are available in [12].

Fig. 2. Arrangement phase and subconductors for the conventional line (red)

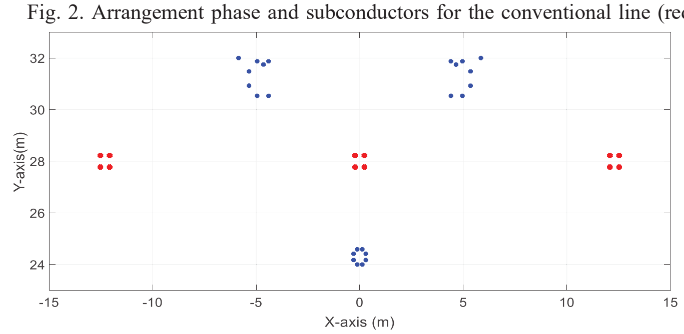

and unconventional HSIL line (blue).

TABLE II. CONDUCTOR INFORMATION AND LINE PARAMETERS FOR THE 17-BUS TEST SYSTEM

Conductor and Bundle Information			Line Parameters	
Type	4 × Macaw		R (Ω/km)	0.0228
Outside diameter of the conductor (inches)	1.055		L (mH/km)	0.878
Subconductor Spacing (m)	0.45		C (nF/km)	12.975

TABLE III. GENERATION, LOAD, AND SHUNT COMPENSATION DATA FOR 17-BUS SYSTEM AT PEAK LOAD

Bus	|V| (p.u)	Type	P_g (MW)	P_L (MW)	Q_L (MW)	Shunt Capacitor
1	1.05	Slack				
2	-	PQ	-	1920.00	929.89	100 Mvar
3	1.05	PV	3600	1750.00	847.56	
4	-	PQ	-	1860.00	900.83	100 Mvar
5	-	PQ	-	1600.00	774.92	100 Mvar
6	1.05	PV	3600	1700.00	823.34	
7	-	PQ	-	1930.00	934.74	50 Mvar
8	1.05	PV	3600	1600.00	774.92	
9	-	PQ	-	2000.00	968.64	350 Mvar
10	1.05	PV	3600	1700.00	823.34	
11	-	PQ	-	1800.00	871.77	200 Mvar
12	1.05	PV	3600	1600.00	774.92	
13	1.05	PV	3600	1800.00	871.77	
14	-	PQ	-	2300.00	1113.94	
15	1.00	PV	3500	1700.00	823.35	
16	-	PQ	-	1740.00	842.72	50 Mvar
17	-	PQ	-	1110.00	537.59	150 Mvar

III. Power Flow Analysis of Test System

AC power flow analysis problem is formulated as

$$I = Y_{bus}V \tag{1}$$

$$P_i + jQ_i = V_i I_i^* \tag{2}$$

$$P_i = |V_i| \sum_{k=1}^{n} |V_k||Y_{ik}|\cos(\delta_i - \delta_k - \theta_{ik}) \tag{3}$$

$$Q_i = |V_i| \sum_{k=1}^{n} |V_k||Y_{ik}|\sin(\delta_i - \delta_k - \theta_{ik}) \tag{5}$$

where, δ_i and $|V_i|$ are the phase angle and magnitude of the voltages at bus i, n is the number of buses in the network, Y_{bus} is the admittance matrix, $|Y_{ik}|$ and θ_{ik} are the magnitude and angle of Y_{ik}, respectively. P_i and Q_i are the injected real and reactive power into the bus i.

$$\text{For normal condition: } 0.95 \le |V_i| \le 1.05\ p.u. \quad (6)$$

$$\text{For contingency condition: } 0.90 \le |V_i| \le 1.05\ p.u. \quad (7)$$

$$-0.3P_{gi} \le Q_{gi} \le 0.6P_{gi} \quad (8)$$

$$S_{ik} \le S_{ik}^{max} \quad (9)$$

Eqs. (6) and (7) represent the voltage constraint in the power system and Eq. (8) is the reactive power generation limit for each generating unit. Eq. (9) is the apparent power flow limit in the transmission line connecting bus i and k. Maximum power flow, S_{ik}^{max}, is determined by the thermal limit of the mentioned line. Using four Macaw conductors per bundle, the thermal limit of the line is $\sqrt{3}$×(500 kV)×(4× 0.870 kA) =3014 MVA. 80% of the thermal limit, 2400 MVA, is considered the line rating, S_{ik}^{max}. The load flow analysis result shown in Table IV indicates that the per unit voltage in all buses, reactive power generation by all generating units, and power flow in all lines are within the defined ranges indicated in Eqs. (6), (8), and (9). This test system can also operate under normal and all single contingencies for peak, dominant, and light load conditions.

TABLE IIII. LOAD FLOW RESULTS FOR THE TEST SYSTEM AT PEAK LOAD UNDER NORMAL OPERATING CONDITION

Bus #	Voltage		Generation	
	$\|V\|$ $p.u.$	δ (deg.)	P_g (MW)	Q_g (Mvar)
1	1.050	0.00	3324.1	-1335.2
2	1.047	-11.63	0.0	0.0
3	1.050	11.44	3600.0	235.7
4	1.047	-15.50	0.0	0.0
5	1.049	-18.80	0.0	0.0
6	1.050	3.12	3600.0	198.3
7	1.042	-19.95	0.0	0.0
8	1.050	-3.31	3600.0	-83.7
9	1.037	-13.39	0.0	0.0
10	1.050	-4.92	3600.0	-117.0
11	1.035	-17.41	0.0	0.0
12	1.050	-9.62	3600.0	-360.5
13	1.050	-4.02	3600.0	285.2
14	1.044	-19.90	0.0	0.0
15	1.000	-5.11	3500.0	-416.7
16	1.050	-19.46	0.0	0.0
17	1.050	-21.21	0.0	0.0

IV. Design of Unconventional HSIL Line

In conventional bundle design, subconductors are symmetrically arranged on a circle in all phases. In contrast, unconventional line bundle conductor design allows subconductors to be placed freely anywhere in space. By shifting phase configurations and subconductors into unconventional arrangements that are geometrically optimized within the space, high natural power designs can be achieved.

Therefore, the optimization problem for designing unconventional HSIL line can be formulated as

$$\text{Objective: Maximize (SIL)} \quad (10)$$

Constraints:

$$E^{max} < E_{pr} \quad (10a)$$

$$D_{ab}^{p2p} > D^{p2p.min} \quad a, b \in \{1,2,3\} \text{ and } a \neq b \quad (10b)$$

$$D_{min}^{p2g} > D_{pr}^{p2g} \quad (10c)$$

$$\text{Symmetry of configuration must be maintained} \quad (10d)$$

The first constraint, Eq. (10a), states that the maximum electric field on the surface of the subconductors, E^{max}, cannot exceed a permissible value, E_{pr}, which is determined by the corona onset gradient. The second constraint, Eq. (10b), indicates that the distance between subconductors of different phases must be greater than the minimum value. The third constraint, Eq. (10c), specifies that the minimum height of sub-conductors above the ground must not exceed a minimum permissible height, D_{pr}^{p2g}. The final constraint ensures symmetrical mechanical loading of the tower. To find the optimal solution for Eq. (10), the initial step involves compacting the configuration to the extent that the maximum electric field intensity approaches its upper limit, E_{pr}. Then, the equalization of phase capacitance is executed to ensure uniformity in the maximum electric field across phases. This allows us to increase SIL in its trade-off with the maximum electric field intensity. The details of capacitance equalization are explained in [8]. After that, the line's compactness is readjusted again to comply with the constraint associated with surface electric field. Finally, the optimal position of each subconductor is determined from its respective candidate positions. Considerations for designing HSIL lines are E_{pr}=20 kV/cm, $D^{p2p.min}$=6.7 m, D_{pr}^{p2g}=24 m, and the maximum height allowed for subconductor = 32 m. The Chickadee conductor, with an outer diameter of 0.743 inches, has been selected in an eight-subconductor bundle per phase. By opting for the Chickadee conductor, which has a smaller outer diameter compared to the Macaw conductor, the unconventional HSIL line incorporating eight Chickadee conductors per bundle maintains an equivalent total Aluminum cross-section and as the conventional line with four Macaw per bundle. In addition, the total weight of the conductors per unit length for both lines is also very close. Therefore, the unconventional HSIL line is cost-comparable to the conventional line. Fig. 2 shows the obtained line configuration for unconventional HSIL lines. The blue dots depict the position of the conductor in each phase. Some specific results and line parameters for this unconventional HSIL line are presented in Table V. In the 500 kV HSIL line proposed in [13], the conductor's maximum height reaches around 38 m from the ground level, accompanied by a line width of approximately 19 m. In [14], the maximum conductor height is 38 m, and the line width is about 13 m. In contrast, for the proposed unconventional HSIL line, the maximum height of conductors and the line width are limited to 32 m and 11.69 m respectively.

TABLE V. IMPORTANT INFORMATION AND LINE PARAMETERS FOR HSIL LINE

Specific Result		Line Parameters	
Maximum Electric Field, E^{max}	20.0 kV/cm	R (Ω/km)	0.0216
Surge Impedance loading	1354.72 MW	L (mH/km)	0.619
Line Width	11.69 m	C (nF/km)	18.199

V. Transmission Expansion Planning (TEP)

The considered transmission expansion planning problem is to supply a 1250 MW load with a power factor of 0.9 lagging at a new bus, referred to as bus 18. For this TEP problem, the system should be capable of operating under normal and all single contingency conditions at different loading conditions – peak load, dominant load, and light load conditions. The nearest buses available to connect the new load are bus#16 and bus #17, located at distances of 324.54 km and 341.83 km, respectively. Assume that the required generation to meet this new load can be provided through the slack bus. And now, we have two transmission technologies, the conventional line, and the unconventional HSIL line, and these can be used for TEP purposes. Initially, the total number of necessary line connections for TEP with each transmission technology is assessed at peak loading conditions. Then, the analysis is conducted to examine the system's requirements and its performance under various loading conditions while maintaining the same line connections.

A. *TEP Using The Conventional Lines*

1) Peak Load

Ensuring the ability of the system to operate under normal conditions and single contingency conditions using conventional lines for TEP necessitates the incorporation of two-line connections from bus#16 and three-line connections from bus#17. Furthermore, an additional line connection from bus 14 to 17 is required to be added to the system. The load flow analysis result for this TEP approach is shown in Fig. 3.

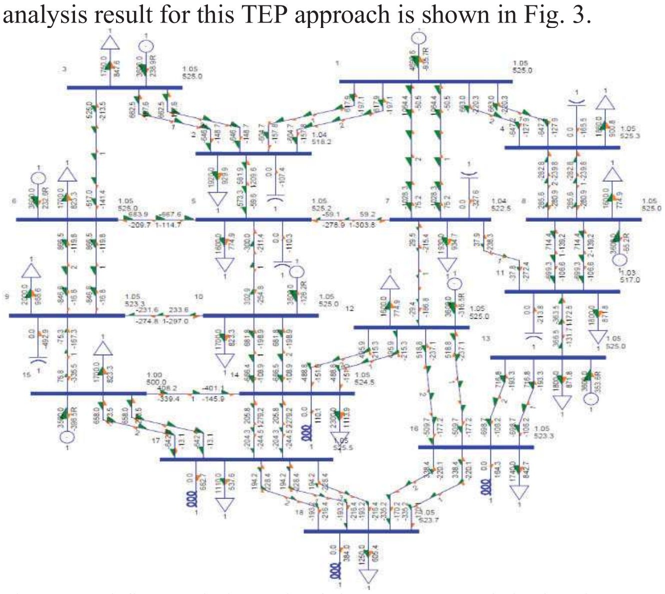

Fig. 3. Load flow analysis result of the system at peak load under normal operating condition when TEP through the conventional line.

A total capacity of 1300 Mvar shunt capacitors and 1200 Mvar shunt reactors are required at different buses to maintain bus voltage and reactive power within the prescribed limit. Power flow in all lines is also within their defined thermal limit. In contingency conditions, the system experiences a minimum voltage of 0.90 p.u. at bus 4 when a line connecting bus 1 and bus 4 is out of operation, this is the worst single contingency case in terms of bus voltage magnitude. Additionally, the maximum loading observed is 68.75% on one of lines 1–7 when the other line 1–7 is not in service. It is noteworthy that the system upholds voltage limits, reactive power generation constraints, and line loading thresholds for all other single contingencies.

2) Dominant Load

The dominant loading condition is considered 60% loading as that of the peak loading condition and the system should be able to satisfactorily operate under normal and single contingency conditions after TEP. For this loading, each generating unit voltage is set to 1.0 p.u. and a total of 3350 Mvar shunt reactors are needed to maintain bus voltage and reactive power generation within the limit. The summarized load flow analysis result after TEP at the dominant load under normal operating conditions is shown in Table VI. During contingency conditions, the minimum voltage observed on the system is at bus 18 with a magnitude of 0.942 p.u. when one line 16–18 goes out of operation. This system meets Eqs. (5)-(8), under both normal and all single contingencies operations.

TABLE VI. LOAD FLOW RESULTS AT DOMINANT LOAD UNDER NORMAL OPERATION THROUGH CONVENTIONAL LINE

Bus #	**Voltage**		**Generation**	
	$\|V\|$ $p.u.$	δ (deg.)	P_g (MW)	Q_g (Mvar)
1	1.000	0.00	3270.3	-1594.4
2	1.039	-13.49	0.0	0.0
3	1.000	-1.44	3600.0	-339.9
4	1.045	-14.01	0.0	0.0
5	1.038	-22.83	0.0	0.0
6	1.000	-11.21	3600.0	-376.5
7	1.020	-21.03	0.0	0.0
8	1.000	-10.12	3600.0	-641.0
9	1.047	-24.67	0.0	0.0
10	1.000	-20.21	3600.0	-573.9
11	1.021	-22.65	0.0	0.0
12	1.000	-25.17	3600.0	-619.3
13	1.000	-20.94	3600.0	-320.4
14	1.044	-33.55	0.0	0.0
15	1.000	-25.78	3500.0	-555.9
16	1.048	-36.28	0.0	0.0
17	1.048	-39.02	0.0	0.0
18	1.046	-43.73	0.0	0.0

3) Light Load

The light loading condition is defined as 40% of peak load, and the power system is expected to function seamlessly under both normal and all single contingency conditions after TEP. In this loading scenario, the voltage for each generating unit is set at 1.0 p.u. and a total of 7650 Mvar shunt reactors need to connect at different buses, then, the system operates well under normal and all single contingency conditions and maintains all the technical requirements such as voltage limit, reactive power generation limits, and line loading limit.

B. *TEP Using Unconventional HSIL Lines*

1) Peak Load

The use of proposed unconventional HSIL lines for the TEP requires two lines from bus 16 to bus 18 and two lines from bus 17 to bus 18 to guarantee the system's ability to operate under normal condition and all single contingencies. Furthermore, it is essential to introduce an additional line connection from bus 14 to bus 17 through the conventional line, like Section A. The load flow analysis result for this TEP approach is shown in Fig. 4. A total capacity of 1300 Mvar shunt capacitors and 1500 Mvar shunt reactors are deployed across various buses to uphold bus voltage and reactive power within the specified limits. Under contingencies, the system encounters a minimum voltage of 0.90 p.u. at bus 4 when one line of 1–4 is switched off and at bus 18 when either one line of 16–18 or 17–18 is out of operation. Additionally, the maximum loading observed is 68.86% on one of lines 1–7 when the other line 1–7 is not in service. Power flow in all lines remains within their specified thermal limit. It is important to highlight that the system operates under normal condition as well as withstands all single contingencies, meeting all technical requirements described in Eqs. (6)-(9).

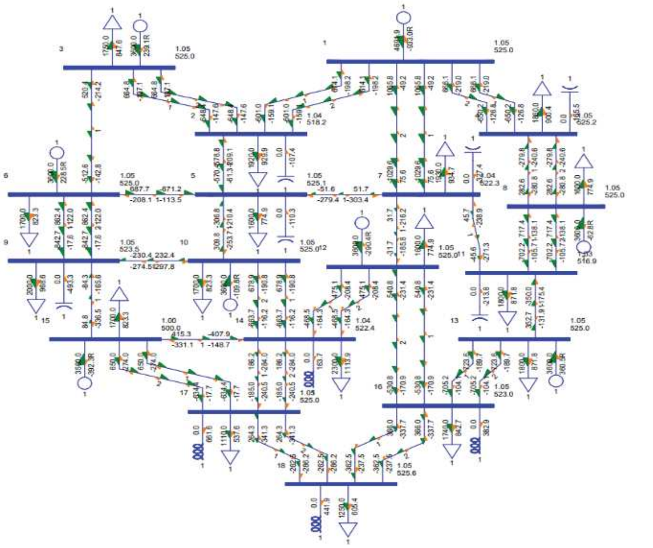

Fig. 4. Load flow analysis result of the system at peak load under normal operating condition when TEP through unconventional HSIL line.

2) Dominant Load

For this loading scenario, each generating unit voltage is set to 1.0 p.u. and a total of 3500 Mvar shunt reactors are needed to maintain bus voltage and reactive power generation within limits. The summarized load flow analysis result after TEP at dominant loading under normal operating conditions is shown in Table VII. In the worst single contingency, the system exhibits a minimum voltage at bus 18 with a magnitude of 0.915 p.u. when one line 17–18 goes out of operation. This system adheres to voltage limits, reactive power generation limits, and line loading thresholds under normal and all contingencies.

3) Light Load

Similar to the TEP scenario with the conventional line under light load conditions, the bus voltage for each generating unit is adjusted to 1.0 p.u. A total capacity of 7950 Mvar shunt reactors is connected to different buses. With this setup for light loading conditions, the system performs effectively under normal and all single contingencies, meeting all the technical requirements such as voltage limits, limits on reactive power generation, and line loading limit, as described in Eqs. (6)-(9). When comparing two transmission technologies—a conventional 500 kV line with a line width of 24.6 m and a surge impedance loading of 996.12 MW, and an unconventional HSIL line with a line width of 11.69 m and surge impedance loading of 1354.72 MW, while keeping the aluminum cross-section constant — for TEP purpose outlined in Section V, the newly designed HSIL line needs a total of four lines and eight 500 kV line bays to connect to substations, as opposed to the conventional line which requires five lines and ten 500 kV line bays in total. Moreover, the ROW needed for the HSIL line is 2.14 times smaller than that required for a conventional line.

TABLE VII. LOAD FLOW RESULTS AT DOMINANT LOAD UNDER NORMAL OPERATION THROUGH UNCONVENTIONAL HSIL LINE

Bus #	Voltage		Generation	
	$\|V\|$ $p.u.$	δ (deg.)	P_g (MW)	Q_g (Mvar)
1	1.000	0.00	3272.5	-1722.1
2	1.049	-13.26	0.0	0.0
3	1.000	-1.15	3600.0	-374.6
4	1.045	-14.26	0.0	0.0
5	1.047	-22.36	0.0	0.0
6	1.000	-10.71	3600.0	-398.9
7	1.042	-20.82	0.0	0.0
8	1.000	-10.14	3600.0	-615.1
9	1.016	-20.04	0.0	0.0
10	1.000	-19.59	3600.0	-619.9
11	1.026	-22.63	0.0	0.0
12	1.000	-24.91	3600.0	-602.9
13	1.000	-21.13	3600.0	-336.9
14	1.050	-32.81	0.0	0.0
15	1.000	-24.82	3500.0	-586.1
16	1.049	-36.64	0.0	0.0
17	1.050	-37.76	0.0	0.0
18	1.045	-42.31	0.0	0.0

VI. Conclusion

This paper presented a detailed analysis of TEP with a conventional line and a proposed unconventional HSIL transmission line having eight subconductors per bundle. These two lines have almost identical total aluminum cross-sections and total conductor weights per unit length. The analysis was performed in a 500 kV power system ensuring system operation under normal and all single contingencies at three different loading conditions. A comparative analysis of the TEP results revealed that the HSIL line required fewer lines and line bays, and a smaller ROW for the same TEP scenario.

References

[1] "Western assessment of resource adequacy", Western Electricity Coordinating Council (WECC), 2022, www.wecc.org/Reliability/2022%20Western%20Assessment%20of%20Resource%20Adequacy.pdf

[2] J. S. Heeter, B. K. Speer, and M. B. Glick, "International best practices for implementing and designing renewable portfolio standard (RPS) policies," Tech. Rep. #NREL/TP-6A20-72798, Apr. 2019.

[3] E. Larson *et al.*, "Net-zero America: Potential pathways, infrastructure, and impacts," interim Rep., Princeton University, Dec. 2020.

[4] F. Kiessling, P. Nefzger, and U. Kaintzyk, *Overhead power Lines, Planning Design, Construction*, Berlin, Germany: Springer, 2003.

[5] Commonwealth of Virginia, Joint Legislative Audit and Review Commission, Evaluation of Underground Electric Transmission Lines in Virginia, House Document No. 87, 2006.

[6] C. L. Bak and F. Faria da Silva, "High voltage AC underground cable systems for power transmission – A review of the Danish experience, part 1," *Electr. Power Syst. Res.*, vol. 140, pp. 984–994, Nov. 2016.

[7] G. Arcia-Garibaldi, P. Cruz-Romero, and A. Gómez-Expósito, "Future power transmission: Visions, technologies and challenges," *Renewable Sustainable Energy Rev.*, vol. 94, pp. 285–301, Oct. 2018.

[8] M. Ghassemi, "High surge impedance loading (HSIL) lines: A review identifying opportunities, challenges, and future research needs," *IEEE Trans. Power Del.*, vol. 34, no.5, pp. 1909–1924, Oct. 2019.

[9] H. Wei-Gang, "Study on conductor configuration of 500 kV Chang-Fang compact line," *IEEE Trans. Power Del.*, vol. 18, no. 3, pp. 1002–8, 2003.

[10] C. K. Arruda *et al.*, "The optimization of transmission lines in Brazil: Proven experience and recent developments in research and development," *IEEE Power & Energy Mag.*, vol. 18, no. 2, pp. 31–42, 2020.

[11] R. G. Olsen and C. Zhuang, "The Spatial Distribution of Electric Field as a Unifying Idea in Transmission Line Design," *IEEE Trans. on Power Del.*, vol. 34, no. 3, pp. 919–928, Jun. 2019.

[12] B. Dhamala, M. Ghassemi, "A high voltage test system meeting requirements under normal and all single contingencies conditions of peak, dominant, and light loadings for transmission expansion planning studies," *IEEE Texas Power and Energy Conf. (TPEC)*, College Station, TX, USA, 2024.

[13] J. S. A. Sarmiento and M. C. Tavares, "Enhancement the overhead transmission lines' capacity by modifying the bundle geometry using heuristics algorithms," *IEEE PES Asia-Pacific Power and Energy Eng. Conf. (APPEEC)*, Xi'an, China, 2016, pp. 646-650.

[14] J. S. Acosta and M. C. Tavares, "Methodology for optimizing the capacity and costs of overhead transmission lines by modifying their bundle geometry," *Electr. Power Syst. Res.*, vol. 163, pp. 668–677, Oct. 2018.